J|A|C|S
ARTICLES
Published on Web 02/10/2006

Heparan Sulfate Degradation via Reductive Homolysis of Its *N*-Chloro Derivatives

Martin D. Rees and Michael J. Davies*

Contribution from the Heart Research Institute, 145-147 Missenden Road, Camperdown, Sydney NSW 2050, Australia

Received November 13, 2005; E-mail: daviesm@hri.org.au

Abstract: The highly basic heme enzyme myeloperoxidase (MPO), which is released by activated phagocytes, catalyzes the production of the potent oxidant hypochlorite (HOCl) from H_2O_2 and chloride ions (Cl^-). Heparan sulfate proteoglycans are key components of the extracellular matrix and cell surfaces and are known to bind MPO avidly via their negatively charged heparan sulfate chains. Reaction of heparan sulfate with HOCl generates polymer-derived *N*-chloro derivatives (chloramines, dichloramines, *N*-chlorosulfonamides, and chloramides). In this study, it is shown that heparan sulfate *N*-chloro derivatives are decomposed in the presence of redox-active transition-metal ions and superoxide ($O_2^{\bullet-}$). These processes initiate polymer modification/fragmentation. Radical intermediates in these processes have been identified by EPR spectroscopy and spin trapping. Evidence has been obtained that the *N*-chloro derivatives undergo reductive homolysis to nitrogen-centered (aminyl, *N*-chloroaminyl, sulfonamidyl, and amidyl) radicals that generate carbon-centered radicals via rapid, intramolecular hydrogen atom abstraction reactions (1,2- and/or 1,5-shifts). In the case of the sulfonamidyl radicals, rearrangement via 1,2-shifts and β-scission of the resultant C-2 carbon-centered radicals to yield $SO_3^{\bullet-}$ and C-2 imines is near quantitative based on the yield of SO_4^{2-}, the decomposition product of $SO_3^{\bullet-}$. The formation of strand breaks and chromophores during these reactions is attributed to the formation and subsequent heterolytic rearrangement of the C-2 imines. The degradation of heparan sulfate via reductive homolysis of its *N*-chloro derivatives may be of significance at sites of inflammation, where MPO-derived HOCl is produced in high concentration and transition-metal ions and $O_2^{\bullet-}$ are known to be present or generated.

Introduction

Heparan sulfate is a member of the glycosaminoglycan family of polysaccharides, which includes hyaluronan, chondroitin sulfate, dermatan sulfate, keratan sulfate, and heparin. Glycosaminoglycans are linear polymers composed of repeating disaccharide subunits that contain a glycosamine residue. They are synthesized in vivo and covalently bound to the core proteins of proteoglycans or, in the case of hyaluronan, as a free polymer.[1] Heparin occurs as a free polymer because of postsynthetic cleavage of the heparin proteoglycan.[2] Heparan sulfate proteoglycans (HSPGs), which are ubiquitous components of the extracellular matrix and cell surfaces, impart important physicochemical properties to basement membranes and are key modulators of cell function and behavior.[3−6] The functions of HSPGs are largely mediated by their glycosaminoglycan chains, and consequently, modification or degradation of such chains may have important biological consequences.

Degradation of HSPGs has been postulated to play a role in a number of inflammatory diseases (e.g., see refs 7 and 8). Leukocytes (neutrophils, monocytes, and macrophages) are key mediators of inflammation-induced tissue damage and may degrade HSPGs at inflammatory foci via the release of proteolytic enzymes, the endoglycosidase enzyme heparanase, or via the production of reactive oxidants such as hypochlorite (HOCl/$^-$OCl, pK_a 7.59;[9] this mixture is henceforth referred to as HOCl).[10] The relative importance of these degradative pathways in vivo is poorly understood. In particular, the susceptibility of heparan sulfate to oxidative degradation has received only limited attention.[10,11]

Activated leukocytes release myeloperoxidase (MPO), a highly basic heme enzyme whose main physiological activity is the production of HOCl. Reaction of the native ferric form of MPO with H_2O_2, the dismutation product of superoxide ($O_2^{\bullet-}$) supplied by the NADPH−oxidase complex of leukocytes and other cells,[12] generates the redox intermediate compound I, which subsequently oxidizes chloride ions (Cl^-) to produce HOCl. As heparan sulfate and other glycosaminoglycans are

(1) Fosang, A. J. In *Extracellular Matrix: Molecular Components and Interactions*; Comper, W. D., Ed.; Harwood Academic: Amsterdam, 1996; Vol. 2, pp 200−229.
(2) Rabenstein, D. L. *Nat. Prod. Rep.* **2002**, *19*, 312−331.
(3) Iozzo, R. V. *Nat. Rev. Mol. Cell Biol.* **2005**, *6*, 646−656.
(4) Fransson, L. A. *Int. J. Biochem. Cell Biol.* **2003**, *35*, 125−129.
(5) Couchman, J. R. *Nat. Rev. Mol. Cell Biol.* **2003**, *4*, 926−937.
(6) Groffen, A. J. A.; Veerkamp, J. H.; Monnens, L. A. H.; van den Heuvel, L. *Nephrol., Dial., Transplant.* **1999**, *14*, 2119−2129.
(7) Kinsella, M. G.; Tran, P. K.; Weiser-Evans, M. C. M.; Reidy, M.; Majack, R. A.; Wight, T. N. *Arterioscler. Thromb. Vasc. Biol.* **2003**, *23*, 608−614.
(8) Rops, A. L.; van der Vlag, J.; Lensen, J. F.; Wijnhoven, T. J.; van den Heuvel, L. P.; van Kuppevelt, T. H.; Berden, J. H. *Kidney Int.* **2004**, *65*, 768−785.
(9) Morris, J. C. *J. Phys. Chem.* **1966**, *70*, 3798−3805.
(10) Klebanoff, S. J.; Kinsella, M. G.; Wight, T. N. *Am. J. Pathol.* **1993**, *143*, 907−917.
(11) Raats, C. J.; Bakker, M. A.; van den Born, J.; Berden, J. H. *J. Biol. Chem.* **1997**, *272*, 26734−26741.
(12) Babior, B. M. *TIBS* **1987**, *12*, 241−243.

Chart 1. *N*-Chloro Derivatives of Glycosamine Monosaccharides and Glycosaminoglycans[a]

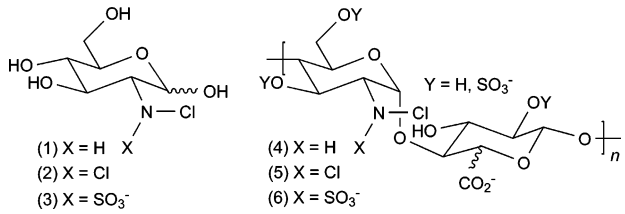

[a] (1) $GlcNH_2$ chloramine; (2) $GlcNH_2$ dichloramine; (3) $GlcNSO_3$ *N*-chlorosulfonamide; (4) polymer-derived chloramines (heparan sulfate and partially de-*N*-sulfated heparin)*; (5) polymer-derived dichloramines (heparan sulfate and partially de-*N*-sulfated heparin)*; (6) polymer-derived *N*-chlorosulfonamides (heparan sulfate, partially de-*N*-sulfated heparin and heparin)*. *The basic repeat unit structures of heparan sulfate and heparin are identical and consist of a variably *N*-substituted β-D-glucosamine residue linked to an uronic acid residue (i.e., β-D-glucuronic acid residue or its epimer α-L-iduronic acid; the latter is more abundant in both polymers[1]). The structures shown do not represent low-energy conformations.

highly negatively charged and form strong electrostatic complexes with the MPO,[13] the production of HOCl is likely to be localized, at least in part, to these materials in vivo.

HOCl has been shown to react with heparan sulfate, heparin, hyaluronan, and chondroitin sulfate via *N*-chlorination of their glycosamine residues.[14,15] Reaction of HOCl with the exclusively *N*-acetylated polymers hyaluronan and chondroitin sulfate yields only chloramides ($R-NCl-C(O)CH_3$). In contrast, heparan sulfate and heparin are variably *N*-substituted, and reaction of HOCl with these polymers can yield a variety of *N*-chloro derivatives. Heparan sulfate and heparin are closely related in structure (cf. Chart 1) and possess *N*-sulfated and *N*-acetylated residues ($GlcNSO_3$ and GlcNAc) in differing proportions; heparan sulfate can possess *N*-unsubstituted residues ($GlcNH_2$). HOCl reacts rapidly with $GlcNH_2$ residues to yield chloramines ($R-NCl-H$, k_2 is ca. 3.1×10^5 M^{-1} s^{-1} at 37 °C), and subsequent reaction of these species yields dichloramines ($R-NCl_2$, k_2 is ca. 9 M^{-1} s^{-1} at 37 °C). Slower reactions occur with $GlcNSO_3$ residues to yield *N*-chlorosulfonamides ($R-NCl-SO_3^-$, k_2 is ca. 0.051 M^{-1} s^{-1} at 37 °C) and with GlcNAc residues to generate chloramides ($R-NCl-C(O)CH_3$, k_2 is ca. 0.012 M^{-1} s^{-1} at 37 °C). Thus, chloramines, dichloramines, and *N*-chlorosulfonamides are formed in preference to chloramides on heparan sulfate.[14] The polymer-derived dichloramines generated on heparan sulfate decompose readily at physiological pH and temperature, with this process initiating cleavage of the polymer backbone.[14] However, the polymer-derived chloramines, *N*-chlorosulfonamides, and chloramides all have long half-lives under these conditions.[14,15]

Elevated levels of transition-metal ions and $O_2^{\bullet-}$ have been shown to be present at sites of inflammation[16,17] and can promote decomposition of chloramides formed on hyaluronan and chondroitin sulfate to give nitrogen-centered (amidyl) radicals via reductive homolysis (i.e., $R-NCl-C(O)CH_3 + e^- \rightarrow R-N^{\bullet}-C(O)CH_3 + Cl^-$).[15,18] These amidyl radicals subsequently initiate site-selective fragmentation of the polymer backbone via intramolecular hydrogen atom abstraction reactions.[15] In light of these data, it was hypothesized that transition-metal ions and $O_2^{\bullet-}$ may also promote degradation of heparan sulfate via decomposition of the *N*-chloro derivatives formed on this polymer upon reaction with HOCl (i.e., primarily chloramines, dichloramines, and *N*-chlorosulfonamides). Evidence is presented here for the occurrence and mechanisms of such reactions, which are distinct from those that underlie the degradation of hyaluronan and chondroitin sulfate.

Experimental Section

Reagents. Solutions were prepared using water filtered through a four-stage Milli Q system. pH control was achieved using 0.1 M phosphate buffer, pH 7.4, treated with washed Chelex resin (Bio-Rad, Hercules, CA) to remove contaminating metal ions. Bovine lung heparin (b-HP), porcine intestinal heparin (p-HP, H-3393), and D-glucosamine hydrochloride ($GlcNH_2$) were from Sigma (St. Louis, MO). Partially de-*N*-sulfated porcine intestine heparin (dnsp-HP) and porcine intestine heparan sulfate (p-HS) were from Celsus Laboratories (Cincinnati, OH). D-[2-^{13}C]-Glucosamine hydrochloride ([2-^{13}C]-$GlcNH_2$) was from Omicron Biochemicals (South Bend, IN). Glucosamine-*N*-sulfate ($GlcNSO_3$) and heparin octasaccharides (from a heparinase I digest of heparin) were from Dextra Laboratories (Reading, U.K.). SOTS-1 (di-(4-carboxybenzyl)hyponitrite) was a gift from Prof. C. Easton (Research School of Chemistry, Australian National University, Canberra, Australia). 5,5-Dimethyl-1-pyrroline *N*-oxide (DMPO) from ICN (Seven Hills, NSW, Australia) was purified before use by treatment with activated charcoal. Stock solutions of 2-methyl-2-nitrosopropane (MNP) were prepared in CH_3CN and diluted into the final reaction mixture such that the final concentration of CH_3CN was $\leq$10% v/v. HOCl solutions were prepared by dilution of a concentrated stock (0.5 M in 0.1 M NaOH) into 0.1 M, pH 7.4, phosphate buffer, with the HOCl concentration determined spectrophotometrically at pH 12 using $\epsilon_{292\ nm}$ 350 M^{-1} cm^{-1}.[9] All other chemicals were of analytical grade. Elimination of O_2 from reaction mixtures was achieved by the use of nitrogen-saturated solutions as described previously.[15]

UV−Vis Spectroscopy. UV−vis spectra were recorded relative to a 0.1 M, pH 7.4, phosphate buffer baseline using a Perkin-Elmer Lambda 40 UV−vis spectrometer.

Determination of *N*-Chloro Derivatives. 5-Thio-2-nitrobenzoic acid (TNB; 35−45 μM in pH 7.4 phosphate buffer) was used to quantify the yield of *N*-chloro derivatives as described previously.[15] With solutions that contained >10 μM Cu^{2+}, EDTA (1 mM) was included to prevent oxidation of TNB by this metal ion. No other reagents employed interfered significantly with the assay.

Computational Modeling. The modeling of the reaction of HOCl with the glycosaminoglycans was performed as described previously with Specfit software[14] using data for the second-order rate constants for reaction of HOCl with each type of glycosamine residue and the content of these residues in the polymers. The second-order rate constants (at 37 °C) used are as follows: reaction with polymer-derived $GlcNH_2$, $k_2 = 3.1 \times 10^5$ M^{-1} s^{-1}; reaction with polymer-derived $GlcNH_2$ chloramines, $k_2 = 9$ M^{-1} s^{-1}; reaction with polymer-derived $GlcNSO_3$, $k_2 = 0.051$ M^{-1} s^{-1}; reaction with polymer-derived GlcNAc, $k_2 = 0.012$ M^{-1} s^{-1}. The glycosamine residue content data used [(a) % $GlcNH_2$, (b) % $GlcNSO_3$, (c) % GlcNAc, (d) calculated disaccharide content of the dry polymer] are as follows: p-HS, (a) 1.7, (b) 43.4, (c) 55.0, (d) 2.13 mmol mg^{-1}; dnsp-HP, (a) 17.1, (b) 71.5, (c) 11.4, (d) 1.66 mmol mg^{-1}; p-HP, (a) 0, (b) 88.6, (c) 11.4, (d) 1.63 mmol mg^{-1}; b-HP, (a) 0, (b) 97.7, (c) 2.3, (d) 1.55 mmol mg^{-1}.

EPR Spectroscopy. EPR spectra were recorded as described previously[15] at room temperature 1−30 min after addition of all reaction

(13) McGowan, S. E. *Am. J. Respir. Cell Mol. Biol.* **1990**, *2*, 271−279.
(14) Rees, M. D.; Pattison, D. I.; Davies, M. J. *Biochem. J.* **2005**, *391*, 125−134.
(15) Rees, M. D.; Hawkins, C. L.; Davies, M. J. *J. Am. Chem. Soc.* **2003**, *125*, 13719−13733.
(16) Stadler, N.; Lindner, R. A.; Davies, M. J. *Arterioscler. Thromb. Vasc. Biol.* **2004**, *24*, 949−954.
(17) Harrison, D.; Griendling, K. K.; Landmesser, U.; Hornig, B.; Drexler, H. *Am. J. Cardiol.* **2003**, *91*, 7A−11A.
(18) Rees, M. D.; Hawkins, C. L.; Davies, M. J. *Biochem. J.* **2004**, *381*, 175−184.

components and/or spin trapped (MNP or DMPO) using a Bruker EMX X-band spectrometer with 100 kHz modulation and a cylindrical ER4103TM cavity. Hyperfine couplings were measured directly from the field scan and confirmed by computer simulation using the program WINSIM (available at http://EPR.niehs.nih.gov). Correlation coefficients between simulated and experimental spectra were >0.95 where the degree of anisotropic line broadening was low; highly broadened spectra gave lower correlation coefficients.

Anion-Exchange Chromatography. Chloride (Cl^-) and sulfate (SO_4^{2-}) were determined by high-performance ion chromatography with suppressed ion conductivity detection using a Dionex Ionpac AS12A (4 mm) analytical column, a Dionex Ionpac AG12A (4 mm) guard column, a Dionex ASRS-Ultra (4 mm) anion self-regenerating suppressor, and a Dionex ED40 electrochemical detector (CD25 shielded conductivity detector). Prior to analysis, samples were diluted 10-fold in water and then filtered (Nanosep centrifugal device, 3000 Da cutoff filter; Pall Life Sciences, Ann Arbor, MI). Samples (10 μL) were eluted at 22 °C at a flow rate of 1.5 mL min^{-1} using a buffer containing 2.7 mM Na_2CO_3 and 0.3 mM $NaHCO_3$ as eluent (Cl^-, $t_R = 3.4$ min; SO_4^{2-}, $t_R = 10.4$ min).

Cation-Exchange Chromatography. Ammonia (NH_4^+) was determined by high-performance ion chromatography with suppressed ion conductivity detection using a Dionex Ionpac CS12A (4 mm) analytical column, a Dionex Ionpac CG12A (4 mm) guard column, a Dionex CSRS-Ultra (4 mm) cation self-regenerating suppressor, and a Dionex ED40 electrochemical detector (CD25 shielded conductivity detector). Prior to analysis, samples were diluted 10-fold in water and then filtered (Nanosep MF GHP centrifugal device, 0.45 μm pore-size filter; Pall Life Sciences, Ann Arbor, MI). Samples (10 μL) were eluted at 22 °C at a flow rate of 1.0 mL min^{-1} using 26 mM methanesulfonic acid (MSA) as eluent (NH_4^+, $t_R = 11.2$ min).

Polyacrylamide Gel Electrophoresis (PAGE). Polymer samples were analyzed using 20% polyacrylamide gels, as described previously.[14] Gels were stained with 0.5% Alcian Blue in 2% CH_3COOH and destained with 2% CH_3COOH. Gel images were acquired using an Umax PowerLook 1120 flatbed scanner and Silverfast Ai 6.0 software (Umax Technologies, Dallas, TX) or using a Bio-Rad Gel Doc 2000 system and Bio-Rad Quantity One software (Bio-Rad, Hercules, CA). Gel images were digitized over a linear range using Bio-Rad Quantity One software (Bio-Rad, Hercules, CA).

Results and Discussion

Preparation of *N*-Chloro Derivatives. *N*-Chloro derivatives of heparan sulfate, partially de-*N*-sulfated heparin, heparin (unmodified), and glycosamine monosaccharides ($GlcNH_2$ and $GlcNSO_3$) were prepared as described previously[14] in 0.1 M phosphate buffer with pH 7.4 by reaction of the parent materials with HOCl (structures are shown in Chart 1). Complete consumption of HOCl was confirmed spectrophotometrically; where excess HOCl was present, it was removed by size-exclusion chromatography. The compositions of the polymer *N*-chloro derivatives were predicted by computational modeling as described previously.[14]

The $GlcNH_2$ chloramine was prepared by reaction of the parent amine (5 mM) with HOCl (1 mM) at 22 °C for 0.5 min. This species was characterized by its distinctive UV−vis absorbance ($\lambda_{max} = 258$ nm) and was shown to be essentially free of the dichloramine ($\lambda_{max} > 300$ nm; see below). The yield of the chloramine was ca. 100% with respect to added HOCl as determined by assay with TNB.

The $GlcNH_2$ dichloramine was prepared by reaction of the parent amine (1 mM) with HOCl (2 mM) at 22 °C for 5 min. The presence of this species was indicated by the formation of an absorbance peak with $\lambda_{max} > 300$ nm. The yield of *N*-chloro derivatives after a 5 min reaction was ca. 32% with respect to added HOCl as determined by assay with TNB.

The $GlcNSO_3$ *N*-chlorosulfonamide was prepared by reaction of $GlcNSO_3$ (10 mM) with HOCl (0.5 mM) at 37 °C for 15 min (ca. 93% yield with respect to added HOCl).

Polymer-derived chloramines were prepared by reaction of porcine intestine heparan sulfate (p-HS; 6.4 mg mL^{-1}) or partially de-*N*-sulfated porcine intestine heparin (dnsp-HP; 6.4 mg mL^{-1}) with HOCl [0.125−0.45 mM (p-HS) and 1.815 mM (dnsp-HP); $HOCl/GlcNH_2$ residues ≤1 in each case] for 0.5 min at 22 °C [ca. 0.1−0.2 mM *N*-chloro derivatives (p-HS) and 1.5 mM *N*-chloro derivatives (dnsp-HP) by assay with TNB]; these preparations are henceforth referred to as p-HS chloramines (>99.9% chloramines by computational modeling) and dnsp-HP chloramines (>99.9% chloramines by computational modeling).

Polymer-derived dichloramines were prepared by reaction of p-HS (6.4 mg mL^{-1}) or dnsp-HP (6.4 mg mL^{-1}) with HOCl (0.45 and 3.63 mM; $HOCl/GlcNH_2$ residues = 2 in each case) for 45 min at 37 °C with subsequent removal of residual HOCl by size-exclusion (PD10) chromatography [ca. 0.16 mM *N*-chloro derivatives (p-HS) and ca. 1.2 mM *N*-chloro derivatives (dnsp-HP) by assay with TNB; chromatography resulted in a 2-fold dilution of the polymers]; these preparations are henceforth referred to as p-HS chloramines (91% dichloramines, 5% chloramines, 2% *N*-chlorosulfonamides, and 2% chloramides by computational modeling) and dnsp-HP dichloramines (94% dichloramines, 3% chloramines, 3% *N*-chlorosulfonamides, and <1% chloramides by computational modeling).

Polymer-derived *N*-chlorosulfonamides were prepared by reaction of bovine lung heparin (b-HP; 6.4 mg mL^{-1}) or porcine intestine heparin (p-HP; 6.4 mg mL^{-1}) with HOCl (40.9 mM) for 16 min at 37 °C with subsequent removal of residual HOCl by size-exclusion (PD10) chromatography (ca. 2.5−2.7 mM *N*-chloro derivatives in each case by assay with TNB); these preparations are henceforth referred to as b-HP NCl (99% *N*-chlorosulfonamides, 1% chloramides by computational modeling) and p-HP NCl (95% *N*-chlorosulfonamides, 5% chloramides by computational modeling).

The stability of the various preparations of *N*-chloro derivatives in the absence of added agents has been examined previously.[14] At 37 °C, slow decomposition occurred with the $GlcNH_2$ chloramine, the $GlcNSO_3$ *N*-chlorosulfonamide, the polymer-derived chloramines, and the polymer-derived *N*-chlorosulfonamides: losses of *N*-chloro derivatives were ca. 0−3% within 60 min incubation (as determined by assay with TNB). Faster decomposition occurred with the $GlcNH_2$ dichloramine and the polymer-derived dichloramines: losses of *N*-chloro derivatives were ca. 70% and ca. 16% within 60 min incubation, respectively (as determined by assay with TNB); complete loss of the $GlcNH_2$ dichloramine absorbance ($\lambda_{max} >$ 300 nm) occurred within this period, and some residual absorbance due to corresponding chloramine ($\lambda_{max} = 258$ nm) was detected.

Decomposition of *N*-Chloro Derivatives by Metal Ions. All of the polymer *N*-chloro derivatives (0.6−1.8 mM in *N*-chloro derivatives) were decomposed upon reaction with Cu^+ [364 μM; generated in situ by the sequential addition of Cu^{2+} (455 μM) and Ti^{3+} (364 μM)] at 22 °C under anoxic conditions for 20 min; Cu^{2+} alone (455 μM) did not stimulate significant

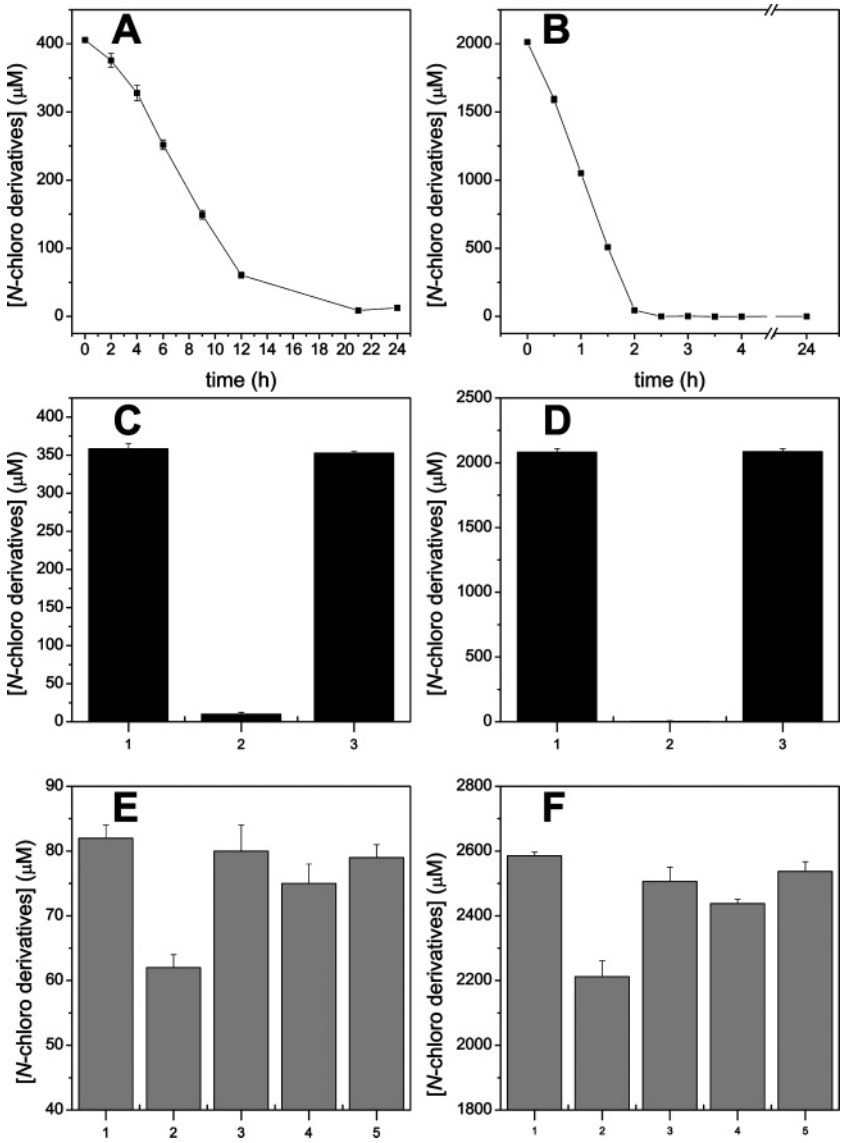

Figure 1. Decomposition of polymer *N*-chloro derivatives by Cu^{2+} and $O_2^{\bullet-}$. *N*-Chloro derivatives were determined by assay with TNB. (A) dnsp-HP chloramines (406 μM) + Cu^{2+} (10 μM), 37 °C, aerobic conditions. (B) p-HP NCl (2.01 mM) + Cu^{2+} (10 μM), 37 °C, aerobic conditions. (C) dnsp-HP chloramines (358 μM) ± Cu^{2+} (10 μM) ± EDTA (100 μM), 37 °C, aerobic conditions, 24 h: column 1, dnsp-HP chloramines; column *2*, dnsp-HP chloramines + Cu^{2+}; column 3, dnsp-HP chloramines + Cu^{2+} + EDTA. (D) p-HP NCl (2.08 mM) ± Cu^{2+} (10 μM) ± EDTA (100 μM), 37 °C, aerobic conditions, 24 h: column 1, p-HP NCl; column 2, p-HP NCl + Cu^{2+}; column 3, p-HP NCl + Cu^{2+} + EDTA. (E) p-HS chloramines (112 μM) ± SOTS-1 (0.67 mM) ± EDTA (100 μM) or SOD (196 U mL^{-1}; 0.05 mg mL^{-1}) or BSA (0.05 mg mL^{-1}), 37 °C, aerobic conditions, 2 h incubation: trace 1, p-HS chloramines; trace 2, p-HS chloramines + SOTS-1; trace 3, p-HS chloramines NCl + SOTS-1+ EDTA; trace 4, p-HS chloramines + SOTS-1 + SOD; trace 5, p-HS chloramines + SOTS-1 + BSA. (F) p-HP NCl (2.59 mM) ± SOTS-1 (0.67 mM) ± EDTA (100 μM) or SOD (196 U mL^{-1}; 0.05 mg mL^{-1}) or BSA (0.05 mg mL^{-1}), 37 °C, aerobic conditions, 2 h incubation: trace 1, p-HP NCl; trace 2, p-HP NCl + SOTS-1; trace 3, p-HP NCl + SOTS-1+ EDTA; trace 4, p-HP NCl + SOTS-1 + SOD; trace 5, p-HP NCl + SOTS-1 + BSA.

decomposition under these conditions. The losses of the *N*-chloro derivatives with respect to added Cu^+ were 33% with the polymer-derived chloramines (dnsp-HP chloramines), 45% with the polymer-derived dichloramines (dnsp-HP chloramines), and 160% with the polymer-derived *N*-chlorosulfonamides (p-HP NCl). Fe^{2+} (364 μM) stimulated extents of decomposition similar to those detected with Cu^+ (data not shown). The Fe^{2+}−EDTA complex (1:1; 364 μM) was ineffective in promoting decomposition; reaction of this negatively charged complex with the polymer-bound *N*-chloro derivatives might be disfavored because of electrostatic repulsion. The monosaccharide *N*-chloro derivatives (0.4−0.9 mM in *N*-chloro derivatives) were also decomposed by Cu^+ (364 μM; generated as above) with losses of 42−135% with respect to added Cu^+.

In incubations at 37 °C under aerobic conditions, Cu^{2+} (10 μM) was found to catalyze decomposition of the polymer-derived chloramines and *N*-chlorosulfonamides (Figure 1A,B). Similar rates of decomposition were observed under anoxic conditions (data not shown). Cu^{2+} (10 μM) did not significantly enhance the rate of decomposition of the polymer-derived dichloramines at 37 °C. Decomposition of the polymer-derived chloramines and *N*-chlorosulfonamides by Cu^{2+} (10 μM) was prevented by EDTA (100 μM) (Figure 1C,D), which is attributed to the formation of a stable, negatively charged, redox-inactive Cu^{2+}−EDTA complex.

Decomposition of the *N*-chloro derivatives by Cu^+ and Fe^{2+} is attributed to one-electron reduction of the N−Cl bond (Scheme 1). With Cu^+ and the polymer-derived *N*-chlorosul-

Scheme 1. Decomposition of Polymer *N*-Chloro Derivatives by Metal Ions and Superoxide Radicals ($O_2^{\bullet-}$)

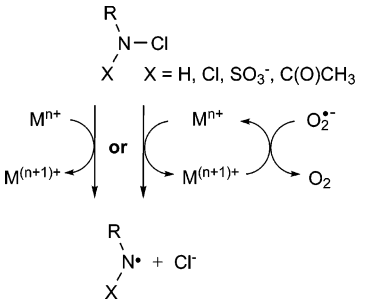

fonamides, the losses that exceeded the concentration of the added metal ion are attributed to the occurrence of chain reactions. Cu^{2+}-catalyzed decomposition of the *N*-chloro derivatives may be initiated via direct, one-electron reduction by Cu^{2+} (cf. evidence for one-electron reduction of hydroperoxides by Cu^{2+} [19]) or via the formation of Cu^{+}. The propagation step in these cyclic redox reactions would involve regeneration of the low-valent state of the metal ion by substrate-derived species (i.e., $Cu^{3+} + e^- \rightarrow Cu^{2+}$ or $Cu^{2+} + e^- \rightarrow Cu^{+}$). Cu^{2+}-catalyzed decomposition of chloramides formed on hyaluronan and chondroitin sulfate has been observed previously;[15] in contrast to Cu^{2+}-catalyzed chloramine/*N*-chlorosulfonamide decomposition, the rates of Cu^{2+}-catalyzed chloramide decomposition were markedly inhibited by O_2.

Decomposition of *N*-Chloro Derivatives by Superoxide. The thermal superoxide ($O_2^{\bullet-}$) source SOTS-1 (di-(4-carboxybenzyl)hyponitrite; $t_{1/2}$ = 4900 s at 37 °C)[20] stimulated the decomposition of p-HS chloramines and p-HP NCl at 37 °C. With p-HP NCl (2.59 mM), the loss of *N*-chloro derivatives induced by SOTS-1 (1.34 mM) was ca. 370 μM, which is ca. 70% of the theoretical yield of $O_2^{\bullet-}$ under these conditions (550 μM[20]). Under the same conditions, decomposition of p-HS chloramines (112 μM) and dnsp-HP chloramines (471 μM) by SOTS-1 (1.34 mM) was less efficient: losses of *N*-chloro derivatives were 53 and 88 μM, respectively. In the absence of added agents, decomposition of the polymer dichloramines was more rapid than production of $O_2^{\bullet-}$ from SOTS-1 and hence an effect of this agent on the rate of dichloramine decomposition could not be determined.

Decomposition of p-HP NCl and p-HS chloramines by SOTS-1 (0.67 mM) was ablated by inclusion of superoxide dismutase (SOD; 196 U mL^{-1}, 0.05 mg mL^{-1}) (Figure 1E,F), and no decomposition was detected with SOTS-1 that had been decomposed by preincubation at 37 °C for 24 h (data not shown). These data demonstrate that decomposition of the *N*-chloro derivatives by SOTS-1 was mediated by $O_2^{\bullet-}$. Inclusion of EDTA (100 μM) and BSA (0.05 mg mL^{-1}) inhibited SOTS-1-induced decomposition of the polymer *N*-chloro derivatives (Figure 1E,F). The effect of these metal ion chelators suggests that reaction of $O_2^{\bullet-}$ with the *N*-chloro derivatives is, at least in part, catalyzed by trace metal ions (e.g., Cu^{2+} and Fe^{3+}; Scheme 1). Binding of such metal ions by EDTA or BSA may disfavor their reduction by $O_2^{\bullet-}$ or disfavor the reaction of their reduced forms with the *N*-chloro derivatives (cf. the effect of EDTA on reaction of Cu^{2+} and Fe^{2+} with the polymer

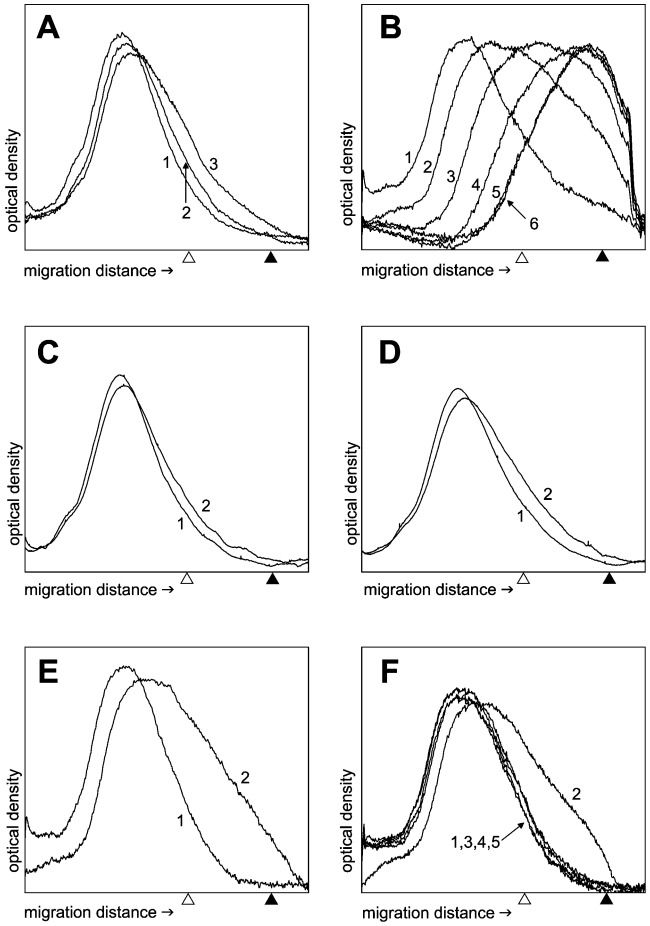

Figure 2. Formation of strand breaks upon decomposition of polymer *N*-chloro derivatives. Polymers were analyzed by PAGE with Alcian Blue staining; densitometric traces of gel lanes are shown. The darts on the horizontal scale indicate the migration positions of the Bromophenol Blue tracking dye (white darts) and the heparin octasaccharide standards (black darts). (A) dnsp-HP chloramines (406 μM) + Cu^{2+} (10 μM), 37 °C, aerobic conditions: trace 1, 0 h; trace 2, 6 h; trace 3, 24 h. (B) p-HP NCl (2.01 mM) + Cu^{2+} (10 μM), 37 °C, aerobic conditions: trace 1, 0 h; trace 2, 0.5 h; trace 3, 1 h; trace 4, 1.5 h; trace 5, 2 h; trace 6, 4 h. (C) dnsp-HP chloramines (622 μM) ± Cu^{+} [364 μM; Cu^{2+} (455 μM) + Ti^{3+} (364 μM)], 22 °C, aerobic conditions, 20 min: trace 1, dnsp-HP chloramines; trace 2, dnsp-HP chloramines + Cu^{+}. (D) dnsp-HP dichloramines (978 μM) ± Cu^{+} [364 μM; as above], 22 °C, aerobic conditions, 20 min: trace 1, dnsp-HP dichloramines; trace 2, dnsp-HP dichloramines + Cu^{+}. (E) p-HP NCl (1.80 mM) ± Cu^{+} [364 μM; as above], 22 °C, aerobic conditions, 20 min: trace 1, p-HP NCl; trace 2, p-HP NCl + Cu^{+}. (F) p-HP NCl (2.59 mM) ± SOTS-1 (0.67 mM) ± EDTA (100 μM) or SOD (196 U mL^{-1}; 0.05 mg mL^{-1}) or BSA (0.05 mg mL^{-1}), 37 °C, aerobic conditions, 24 h incubation: trace 1, p-HP NCl; trace 2, p-HP NCl + SOTS-1; trace 3, p-HP NCl + SOTS-1+ EDTA; trace 4, p-HP NCl + SOTS-1 + SOD; trace 5, p-HP NCl + SOTS-1 + BSA.

N-chloro derivatives). Inhibition of $O_2^{\bullet-}$-mediated decomposition of hyaluronan- and chondroitin-sulfate-derived chloramides by EDTA and BSA has previously been ascribed to their ability to inactivate catalytic metal ions.[15]

Formation of Strand Breaks. Changes in the molecular mass of the polymers upon reaction with the metal ions and $O_2^{\bullet-}$ were assessed by polyacrylamide gel electrophoresis (PAGE) with Alcian Blue staining (Figure 2). In the absence of added agents at 37 °C, significant polymer fragmentation was observed within 24 h of incubation with the polymer-derived dichloramines (p-HS dichloramines and dnsp-HP dichloramines) but not with the polymer chloramines, *N*-chlorosulfonamides and chloramides (p-HS chloramines, dnsp-HP chloramines, p-HP

(19) Jones, C. M.; Burkitt, M. J. *J. Am. Chem. Soc.* **2003**, *125*, 6946−6954.
(20) Ingold, K. U.; Paul, T.; Young, M. J.; Doiron, L. *J. Am. Chem. Soc.* **1997**, *119*, 12364−12365.

NCl, and b-HP NCl) (data not shown). This accords with the rate and extent of decomposition of these *N*-chloro derivatives under these conditions and is consistent with previous data.[14]

Decomposition of p-HP NCl by Cu^{+} at 22 °C under anoxic conditions resulted in extensive polymer fragmentation (Figure 2E); similar data were obtained with b-HP NCl (data not shown). Slightly less-extensive fragmentation was observed with Fe^{2+} (data not shown). Decomposition of dnsp-HP chloramines and dnsp-HP dichloramines by Cu^{+} also resulted in polymer fragmentation (Figure 2C,D). No fragmentation was detected in equivalent experiments with the parent polymers or where the *N*-chloro derivatives were quenched by prior reaction with methionine (data not shown). Fe^{2+}−EDTA, which was ineffective in inducing *N*-chloro derivative decomposition, did not induce significant polymer fragmentation (data not shown).

Decomposition of dnsp-HP chloramines and p-HP NCl by Cu^{2+} (10 μM) at 37 °C and pH 7.4 resulted in time-dependent depolymerization (Figure 2A,B) consistent with the rate and extent of *N*-chloro derivative decomposition detected in these incubations (cf. Figure 1A,B); experiments with b-HP NCl (not shown) gave data similar to those obtained with p-HP NCl. The exclusion of oxygen did not affect the rate or extent of fragmentation induced by Cu^{2+} (data not shown). As with Cu^{+}-induced decomposition, no fragmentation was detected in equivalent experiments with the parent polymers or where the *N*-chloro derivatives were quenched by prior reaction with methionine (data not shown). Inclusion of EDTA prevented polymer fragmentation (data not shown), consistent with the protective effect that EDTA exerted against *N*-chloro derivative decomposition (cf. Figure 1D).

The average degree of polymerization (DP) of the fragments generated upon complete decomposition of p-HP NCl (2.01 mM) was estimated to be ca. 8 by comparison to purified heparin octasaccharides (DP = 8, obtained via heparinase-I cleavage of heparin; cf. Figure 2B). The molecular mass of p-HP is ca. 17−19 kDa (data from supplier), which is equivalent to a DP of 55−62 (average molecular mass of disaccharides: 614 Da[14]). Using these data, and the concentration of the parent polymer (2.91 mg mL^{-1}, accounting for dilution after PD10 chromatography and addition of Cu^{2+}), we calculated the yield of strand breaks to be up to ca. 50% with respect to loss of *N*-chloro derivatives (eqs 1−3). This may be an underestimate, as strand scission is accompanied by a loss of charge density (see Formation of Sulfate section below), and the resulting fragments would therefore be expected to have a lower electrophoretic mobility than those generated via enzymatic cleavage.

$$\text{strand breaks per chain} = (\text{initial DP}/\text{final DP}) - 1 \quad (1)$$

$$\textit{N}\text{-chloro derivatives lost per chain} = [\textit{N}\text{-chloro derivatives lost}]\ (\text{mol L}^{-1})/[\text{chains}]\ (\text{mol L}^{-1}) \quad (2)$$

$$[\text{chains}]\ (\text{mol}) = [\text{parent polymer}]\ (\text{g L}^{-1})/\text{initial molecular mass of parent polymer}\ (\text{g mol}^{-1}) \quad (3)$$

Exposure of p-HP NCl to SOTS-1 at 37 °C resulted in polymer fragmentation (Figure 2F). No fragmentation was detected in equivalent experiments with the parent polymer or where the *N*-chloro derivatives were quenched by prior reaction with methionine (data not shown). The polymer fragmentation induced by SOTS-1 was ablated by prior decomposition of the SOTS-1 (data not shown) and by inclusion of SOD, EDTA, or BSA (Figure 2F). This accords with the inhibitory effect of these agents against *N*-chloro derivative decomposition (cf. Figure 1F). The preceding data are consistent with SOTS-1-induced fragmentation occurring via $O_2^{\bullet-}$-dependent, metal-ion-catalyzed, one-electron reduction of the *N*-chloro derivatives to nitrogen-centered radicals (cf. Scheme 1). With the polymer-derived chloramines, which only decompose to a limited extent in the presence of SOTS-1, fragmentation could not be detected, by PAGE, in the presence of this agent (data not shown).

Formation of Radicals. Transition-metal ions and $O_2^{\bullet-}$ have been shown to initiate polymer fragmentation by decomposition of the *N*-chloro derivatives, and these reactions are postulated to involve the initial formation of nitrogen-centered radicals (Scheme 1). The formation of these, and other, radicals from monosaccharide and polymer *N*-chloro derivatives was investigated by EPR spectroscopy with spin trapping, using MNP and DMPO as spin traps. Where radical formation from the *N*-chloro derivatives was detected, no radical formation was detected in equivalent experiments (i) with the corresponding parent compounds, (ii) where the *N*-chloro derivatives were quenched by prior reaction with excess methionine, or (iii) where the spin trap was omitted from the reaction mixture. Spectral data for all the species detected, together with assignments, are given in Tables 1 and 2 (Supporting Information). The latter are based on observed splitting patterns and comparison of the hyperfine coupling constants with data for related species[15] (see also: http://EPR.niehs.nih.gov/stdb). The measured hyperfine coupling constants were confirmed by computer simulation.

A. $GlcNH_2$ Chloramine. Reaction of Cu^{+} [327 μM; i.e., Cu^{2+} (408 μM)/Ti^{3+} (327μM)] with the [2-^{13}C]−$GlcNH_2$ chloramine (ca. 800 μM) in the presence of DMPO (102 mM) at ca. 22 °C under anoxic conditions resulted in the detection of three carbon-centered radical adduct signals [(i) a(N, NO) = 1.55, $a(\beta$-H) = 2.50, $a(\gamma$-^{13}C) = 0.66 mT; (ii) a(N, NO) = 1.56, $a(\beta$-H) = 2.34, $a(\gamma$-^{13}C) = 0.67 mT; (iii) a(N, NO) = 1.53, $a(\beta$-H) = 2.28, $a(\gamma$-^{13}C) = 0.80 mT] (Figure 3A,B). Signals detected with the (unlabeled) $GlcNH_2$ chloramine were identical but lacked the ^{13}C couplings (data not shown). With the [2-^{13}C]-labeled derivative, the presence of a large ^{13}C coupling [$a(\gamma$-^{13}C) = 0.66−0.80 mT] in each of the signals detected is consistent with their assignment to isomeric adducts of a single radical, the $GlcNH_2$ C-2 carbon-centered radical. The total intensity of these signals (determined by double integration) was greatest in the first spectrum acquired (i.e., within 2 min of addition of the metal ions), consistent with rapid decomposition of the $GlcNH_2$ chloramine. Over time, one of the isomeric C-2 adducts increased in abundance relative to the others (data not shown). This phenomenon, which has been observed previously with isomeric DMPO adducts and MNP adducts of the GlcNAc C-2 carbon-centered radical,[14,15] is attributed to the presence of adduct isomers (i.e., anomers and a ring-open form) that interconvert over time via mutarotation. In the absence of added metal ions, the same signals were detected but in lower intensity. In equivalent experiments with MNP (20.4 mM) as the spin trap, no substrate-derived signals were detected. Inefficient trapping of the $GlcNH_2$ C-2 carbon-centered radical by MNP is likely to involve electronic rather

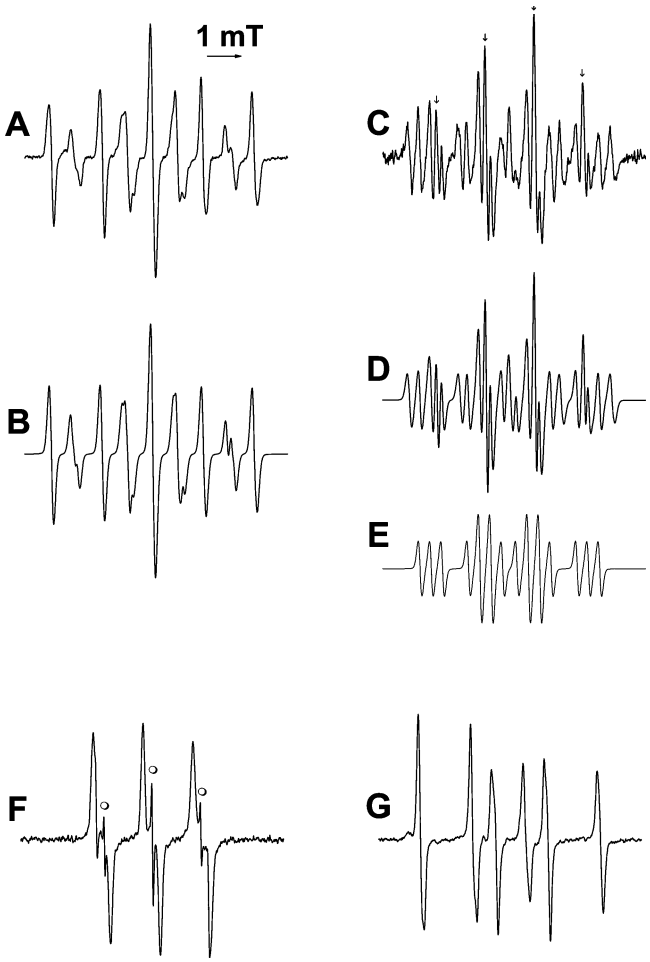

Figure 3. EPR spectra of spin adducts detected on decomposition of monosaccharide *N*-chloro derivatives in the presence of Cu^+. The *N*-chloro derivatives (ca. 290−800 μM) were incubated with Cu^+ (327 μM) at ca. 22 °C under anoxic conditions in the presence of DMPO (102 mM) or MNP (20.4 mM). (A) [2-^{13}C]−$GlcNH_2$ chloramine, Cu^+, DMPO, after 1 min reaction. (B) Computer simulation of spectrum in (A) using the following components: three isomeric adducts of the [2-^{13}C]−$GlcNH_2$ C-2 carbon-centered radical [(i) a(N, NO) = 1.55, a(β-H) = 2.50, a(γ-^{13}C) = 0.66 mT; (ii) a(N, NO) = 1.56, a(β-H) = 2.34, a(γ-^{13}C) = 0.67 mT; (iii) a(N, NO) = 1.53, a(β-H) = 2.28, a(γ-^{13}C) = 0.80 mT]. (C) [2-^{13}C]−$GlcNH_2$ dichloramine, Cu^+, DMPO, after 1 min reaction. (D) Computer simulation of spectrum in (C) using the following components: the adduct of the $GlcNH_2$ *N*-chloroaminyl radical [a(N, NO) = 1.48, a(β-H) = 1.83, a(γ-N) = 0.34 mT], three isomeric adducts of the [2-^{13}C]−$GlcNH_2$ C-2 carbon-centered radical [parameters as above], and DMPO−OH [a(N, NO) = 1.49, a(β-H) = 1.49 mT]. (E) Simulated spectrum of the adduct of the $GlcNH_2$ *N*-chloroaminyl radical [a(N, NO) = 1.48, a(β-H) = 1.83, a(γ-N) = 0.34 mT]. (F) $GlcNSO_3$ *N*-chlorosulfonamide, Cu^+, MNP, after 19 min reaction; ○ = MNP−SO_3^- [a(N, NO) = 1.47 mT]. (G) $GlcNSO_3$ *N*-chlorosulfonamide, Cu^+, DMPO, after 1 min reaction.

than steric factors given that MNP traps the more hindered C-2 radicals derived from GlcNAc[15] and $GlcNSO_3$ (see below) and that the $GlcNH_2$ C-2 radical is trapped by the bulkier spin trap DMPO. Electronic factors have previously been shown to inhibit trapping of related carbon-centered radicals by MNP.[21]

Formation of the $GlcNH_2$ C-2 carbon-centered radical upon addition of Cu^+ is attributed to an intramolecular 1,2-hydrogen atom shift to an initial (undetected) aminyl radical, produced via one-electron reduction of the chloramine (Scheme 2); an analogous 1,2-shift has been observed previously with the

Scheme 2. Proposed Reactions of Monosaccharide-Derived Nitrogen-Centered Radicals

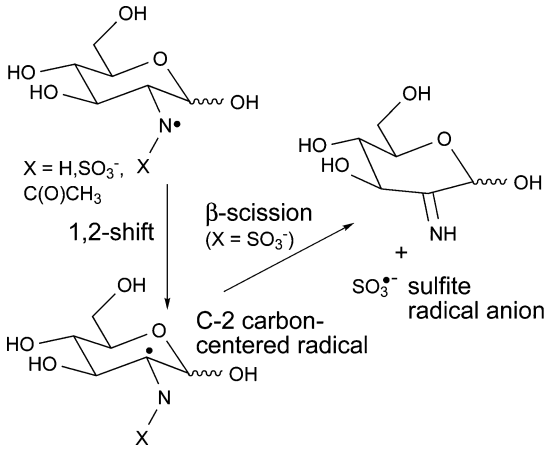

GlcNAc amidyl radical (Scheme 2).[15] Radical formation in the absence of added metal ions may be promoted by one-electron reductants derived from sugar autoxidation.[22]

B. $GlcNH_2$ Dichloramine. Reaction of Cu^+ (327 μM; prepared as above) with the [2-^{13}C]−$GlcNH_2$ dichloramine (ca. 530 μM) in the presence of DMPO (102 mM) at 22 °C under anoxic conditions resulted in the detection of a nitrogen-centered radical adduct [a(N, NO) = 1.48, a(β-H) = 1.83, a(γ-N) = 0.34 mT] and three weak signals due to adducts of the C-2 carbon-centered radical (with parameters identical to those detected with the [2-^{13}C]−$GlcNH_2$ chloramine; see above) (Figure 3C−E). In the absence of added metal ions, the same signals were detected but in lower intensity. In equivalent experiments with MNP (20.4 mM) as the spin trap, no substrate-derived signals were detected.

The nitrogen-centered radical detected upon addition of Cu^+ is postulated to be an *N*-chloroaminyl radical, produced via one-electron reduction of the dichloramine. As with the corresponding chloramine, radical formation in the absence of added metal ions may be promoted by one-electron reductants derived from sugar autoxidation. The C-2 carbon-centered radical trapped in low yield in these experiments may arise from decomposition of chloramine present in low levels in these reaction mixtures.

C. $GlcNSO_3$ *N*-Chlorosulfonamide. Reaction of Cu^+ (327 μM; prepared as above) with the $GlcNSO_3$ *N*-chlorosulfonamide (ca. 290 μM) in the presence of MNP (20.4 mM) at ca. 22 °C under anoxic conditions resulted in the detection of a signal assigned to the adduct of $SO_3^{\bullet-}$ (sulfite radical anion) [a(N) = 1.47 mT]; this was confirmed by generating authentic MNP−SO_3^- via autoxidation of an air-saturated solution of Na_2SO_3 (100 mM) and MNP (20.4 mM) at 22 °C. Three substrate-derived carbon-centered radical adducts were also detected [(i) a(N, NO) = 1.52, a(γ-H) = 0.05, a(β-N) = 0.18 mT; (ii) a(N, NO) = 1.53, a(N) = 0.18 mT; (iii) a(N, NO) = 1.50, a(γ-H) = 0.08, a(β-N) = 0.22 mT] (Figure 3F). The presence of a large, substrate-derived nitrogen coupling [a(β-N) = 0.18−0.22 mT] in each of the carbon-centered radical adduct signals is consistent with their assignment to isomeric adducts of a single radical, the $GlcNSO_3$ C-2 carbon-centered radical. Similarly large, substrate-derived nitrogen couplings [a(β-N) = 0.26−0.30 mT] have been detected in the signals of the MNP adducts of the

(21) Madden, K. P.; Taniguchi, H. *J. Chem. Soc., Perkin Trans. 2* **1993**, *11*, 2095−2103.

(22) Thornalley, P. J. *Environ. Health Perspect.* **1985**, *64*, 297−307.

GlcNAc C-2 carbon-centered radical.[15] With the $GlcNSO_3$ C-2 adducts, the total signal intensity was greatest in the first acquired spectrum. Over time, one of these species accumulated at the expense of the others (data not shown); this is attributed, as above, to interconversion of adduct isomers via mutarotation. With DMPO (102 mM) as the spin trap, three carbon-centered radical adducts were detected [(i) a(N, NO) = 1.61, $a(\beta$-H) = 2.33 mT; (ii) a(N, NO) = 1.61, $a(\beta$-H) = 2.14 mT; (iii) a(N, NO) = 1.54, $a(\beta$-H) = 2.31 mT] (Figure 3G). These signals are assigned to isomeric adducts of the $GlcNSO_3$ C-2 carbon-centered radical.

Formation of the $GlcNSO_3$ C-2 carbon-centered radical upon addition of Cu^+ is attributed to an intramolecular 1,2-hydrogen shift to an initial sulfonamidyl radical, produced via one-electron reduction of the *N*-chlorosulfonamide; the formation of $SO_3^{\bullet-}$ is attributed to subsequent β-scission of the C-2 species (i.e., $R^{\bullet}-NH-SO_3^- \rightarrow R{=}NH + SO_3^{\bullet-}$) (Scheme 2).

D. Polymer-Derived Chloramines. Reaction of Cu^+ (327 μM; prepared as above) with dnsp-HP chloramines (ca. 560 μM) in the presence of DMPO (102 mM) at ca. 22 °C under anoxic conditions resulted in the detection of a signal due to the adduct of $CO_2^{\bullet-}$ (carboxyl radical anion) [a(N, NO) = 1.57, $a(\beta$-H) = 1.86 mT] and broad signals due to carbon-centered radical adducts [a(N, NO) = ca. 1.57, $a(\beta$-H) = ca. 2.34 mT] (Figure 4A). These signals were most intense in the first spectrum acquired, i.e., within 2 min of addition of the metal ions. With p-HS chloramines, identical though slightly sharper carbon-centered radical adduct signals were detected along with the $CO_2^{\bullet-}$ adduct. In equivalent experiments with dnsp-HP chloramines and p-HS chloramines using MNP (20.4 mM) as the spin trap, no substrate-derived signals were detected. The carbon-centered species trapped by DMPO under these conditions may be trapped inefficiently by MNP. No substrate-derived radicals were detected in the absence of added metal ions under any of the preceding reaction conditions.

The generation of radicals from p-HS and dnsp-HP chloramines is ascribed to decomposition of these species to aminyl radicals via one-electron reduction. Studies of molecular models suggest that the polymer-derived aminyl radicals may undergo intramolecular 1,5-hydrogen atom shifts to yield uronic-acid-derived (IdoA- and/or GlcA-derived) C-4 carbon-centered radicals in addition to 1,2-hydrogen shifts to yield $GlcNH_2$-derived C-2 carbon-centered radicals (Scheme 3). Other intramolecular reactions of these radicals are predicted to be disfavored because of stereochemical restraints. The generation of $CO_2^{\bullet-}$ is attributed to β-scission of these C-4 carbon-centered radicals (Scheme 3). Evidence has been obtained in previous studies for the occurrence of analogous $CO_2^{\bullet-}$-yielding β-scission reactions of GlcA-derived C-4 carbon-centered radicals formed on hyaluronan and chondroitin sulfate.[15]

E. Polymer-Derived Dichloramines. Reaction of Cu^+ (327 μM; prepared as above) with dnsp-HP dichloramines (ca. 980 μM) in the presence of DMPO (102 mM) at 22 °C under anoxic conditions resulted in the detection of very weak, broad signals that are assigned to adducts of polymer-derived radicals (Figure 4B). The hyperfine coupling constants of these signals could not be measured accurately. Rapid decay of these EPR signals confounded the use of enzymatic digestion (0.1 U mL^{-1} heparinase II, 37 °C) to enhance signal resolution via the release of more mobile fragments. In the absence of added metal ions at 22 °C, no substrate-derived radical adducts were detected. With Cu^+ and MNP as the spin trap, no substrate-derived radicals were detected. A weak signal due to the adduct of $SO_3^{\bullet-}$ [a(N, NO) = 1.47 mT] was detected upon incubation of dnsp-HP dichloramines with Cu^{2+} (100 μM) at 37 °C in the presence of MNP (20.4 mM) for 30 min prior to spectral acquisition. No substrate-derived radicals were detected in the absence of added metal ions under any of these reaction conditions.

Reaction of Cu^+ with the polymer-derived dichloramines would be expected to generate *N*-chloroaminyl radicals (cf. generation of the $GlcNH_2$ *N*-chloroaminyl radical upon reaction of Cu^+ with the $GlcNH_2$ dichloramine; see above). The polymer-

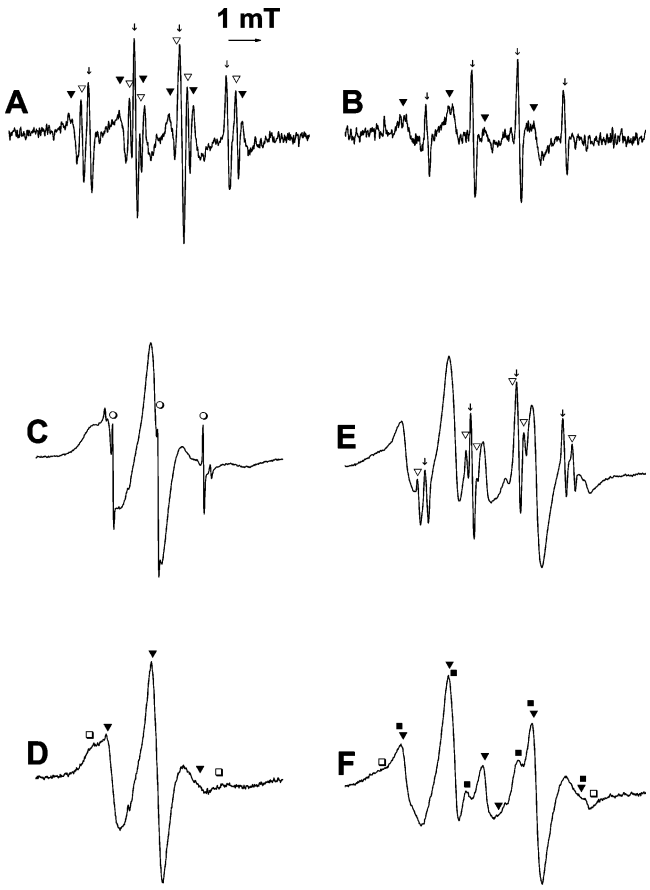

Figure 4. EPR spectra of spin adducts detected on decomposition of polymer *N*-chloro derivatives in the presence of Cu^+. The *N*-chloro derivatives (0.56−1.8 mM) were incubated with Cu^+ (327 μM) at ca. 22 °C under anoxic conditions in the presence of DMPO (102 mM) or MNP (20.4 mM). (A) Polymer-derived chloramines (dsnp-HP chloramines), Cu^+, DMPO, after 1 min reaction; ▼ = polymer-derived carbon-centered radical adducts [a(N, NO) = ca. 1.57, $a(\beta$-H) = ca. 2.34 mT], ▽ = DMPO−CO_2^- [a(N, NO) = 1.57, $a(\beta$-H) = 1.86 mT], ↓ = DMPO−OH [a(N, NO) = 1.49, $a(\beta$-H) = 1.49 mT]. (B) Polymer-derived dichloramines (dsnp-HP dichloramines), Cu^+, DMPO, after 1 min reaction; ▼ = features due to unidentified species [parameters unknown; cf. signals in (F)], ↓ = DMPO−OH [parameters as above]. (C) Polymer-derived *N*-chlorosulfonamides (p-HP NCl), Cu^+, MNP, after 1 min reaction; ○ = MNP−SO_3^- [a(N, NO) 1.47 mT]. (D) Reaction mixture as in (C), high-molecular mass fraction eluted from size-exclusion (PD10) column; □ = adduct of carbon-centered radical [a(N, NO) > 1.50 mT], ▼ = adduct of carbon-centered radical [a(N, NO) ca. 1.50 mT]. (E) Polymer-derived *N*-chlorosulfonamides (b-HP NCl), Cu^+, DMPO, after 1 min reaction; ▽ = DMPO−CO_2^- [parameters as above], ↓ = DMPO−OH [parameters as above]. (F) Reaction mixture as in (E), high-molecular mass fraction eluted from size-exclusion (PD10) column; ▼ = carbon-centered radical [a(N, NO) = ca. 1.50, $a(\beta$-H) = ca. 2.70 mT. Lines indicated with □ and ■ are from unidentified species.

Scheme 3. Proposed Reactions of Polymer-Derived Nitrogen-Centered Radicals[a]

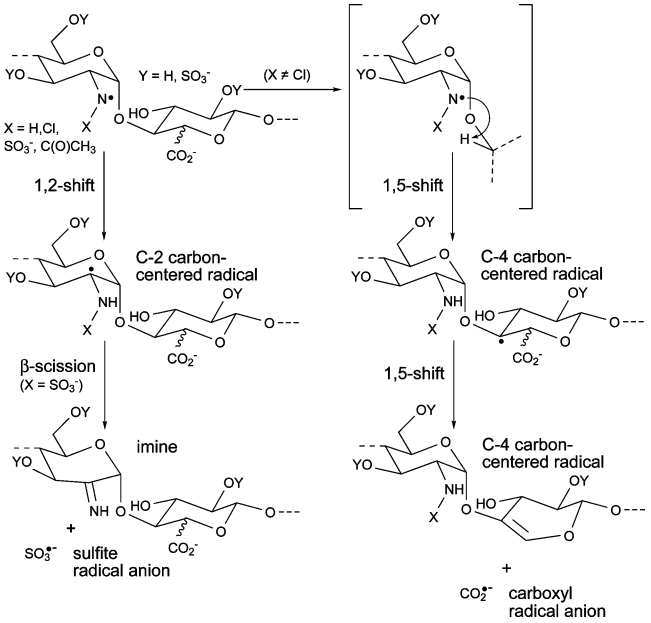

[a] Extensions of the partial structures shown are indicated by dashed bonds.

derived DMPO adducts detected could be adducts of these nitrogen-centered radicals or adducts of carbon-centered radicals generated via their rearrangement (e.g., via 1,2- and 1,5-shifts; as with the corresponding aminyl radicals, the study of molecular models suggests that there are no stereochemical impediments to these reactions). However, the species detected may also be formed via reaction of Cu^+ with other *N*-chloro derivatives present in low abundance in the reaction mixture such as *N*-chlorosulfonamides (3% of *N*-chloro derivatives). Consistent with this proposal, the polymer-derived DMPO adducts detected are similar to those detected with the polymer-derived *N*-chlorosulfonamides (cf. Figure 4B and Figure 4E,F and below). The MNP adduct of $SO_3^{\bullet-}$ detected upon incubation with Cu^{2+} is also likely to arise from decomposition of polymer-derived *N*-chlorosulfonamides (see below). Thus, although *N*-chloroaminyl radicals may be generated in the above reaction systems, these species may not form observable adducts. As $CO_2^{\bullet-}$ was not detected, it appears that the *N*-chloroaminyl 1,5-shifts which would yield this species do not occur (cf. detection of $CO_2^{\bullet-}$ from the polymer-derived chloramines).

F. Polymer-Derived *N*-Chlorosulfonamides. Reaction of Cu^+ (327 μM) with p-HP NCl (ca. 1.8 mM) at 22 °C in the presence of MNP (20.4 mM) under anoxic conditions resulted in the detection of the $SO_3^{\bullet-}$ adduct [a(N, NO) = 1.47] and long-lived, broad signals assigned to adducts of polymer-derived carbon-centered radicals (Figure 4C). Identical spectra were obtained with b-HP NCl (data not shown). The intensity of these signals was greatest in the first spectrum acquired, i.e., within 2 min of addition of the metal ions. The same signals were observed upon incubation of p-HP NCl with Cu^{2+} (100 μM) at 37 °C in the presence of MNP (20.4 mM) for 30 min prior to spectral acquisition; similar signal intensities were observed in anoxic and aerobic incubations. With Cu^+ at 22 °C under anoxic conditions using DMPO as the spin trap, the $CO_2^{\bullet-}$ adduct [a(N, NO) = 1.57, $a(\beta$-H) = 1.86 mT] was detected along with broad signals assigned to adducts of polymer-derived radicals (Figure 4E). In experiments with Fe^{2+} (327 μM) at 22 °C using MNP and DMPO as spin traps, adducts were detected that were identical to those detected with Cu^+, though maximal radical adduct yields were not achieved until after 30 min of reaction. No substrate-derived radicals were detected in the absence of added metal ions under any of the preceding reaction conditions.

The polymer-derived radical adducts detected with MNP and DMPO coeluted with the intact polymers on size-exclusion (PD10) chromatography. This treatment removed low-molecular mass paramagnetic species (i.e., MNP$-SO_3^-$, DTBN, DMPO$-CO_2^-$, and DMPO$-$OH) and facilitated analysis of the signals due to the polymer-derived adducts (Figure 4D,F). Spectra of the purified MNP adducts (Figure 4D) showed the presence of a major signal with a triplet hyperfine splitting [a(N, NO) = ca. 1.50 mT] and a minor signal detected as broad shoulders on the outside of the lines due to the major signal. Digestion of the polymer-derived adducts with heparinase II (0.1 U mL^{-1}, 37 °C, 2 h) resulted in a slight increase in the sharpness of the signals, consistent with the release of more mobile low-molecular mass adduct fragments (data not shown). However, despite this treatment, these signals were insufficiently resolved to allow accurate measurement of hyperfine coupling constants. The minor signal appeared to consist of a triplet coupling arising from the nitroxide nitrogen [i.e., a(N, NO) > 1.50 mT]; the presence of an additional, unresolved hyperfine coupling could not be excluded.

Spectra of the purified DMPO adducts (Figure 4F) showed the presence of a signal due to a carbon-centered radical adduct [a(N, NO) = ca. 1.50, $a(\beta$-H) = ca. 2.70 mT] and two other unassigned signals, one of which appears to possess an unusually large nitroxide nitrogen coupling [a(N, NO) = ca. 2.10, $a(\beta$-H) = ca. 1.7 mT]. The species that give rise to these signals have not been identified. Only the outermost features of the other unidentified radical could be discerned; the measured distance between these features was ca. 7.0 mT. Attempts to improve the resolution of the signals, and thus their characterization, by digestion of the adducts with heparinase II (as above) were confounded by adduct instability.

The initiation of radical formation from b-HP NCl and p-HP NCl is ascribed primarily to the decomposition of *N*-chlorosulfonamides to sulfonamidyl radicals via one-electron reduction. Formation of amidyl radicals from chloramides, which are predicted to be present in low abundance (1−5%), may represent a minor pathway to radical generation. It is unlikely that any of the polymer-derived adducts detected are adducts of the initial nitrogen-centered radicals, as it has been shown that DMPO does not form detectable adducts with the corresponding monosaccharide-derived radicals, i.e., the $GlcNSO_3$ sulfonamidyl radical (see above) and the GlcNAc amidyl radical,[15] and trapping of the polymer-derived species is unlikely to be more efficient. Studies of molecular models suggest that the polymer-derived sulfonamidyl radicals and amidyl radicals may undergo (rapid) 1,2- and 1,5-shifts (Scheme 3). All of the polymer-derived adducts detected are likely to be adducts of carbon-centered radicals generated via these reactions; these assignments are tentative in some cases because of atypical/undetermined hyperfine coupling constants (see above). Both 1,2- and 1,5-shifts have been observed previously with the amidyl radical derived from the GlcNAc α-methyl glycoside, a

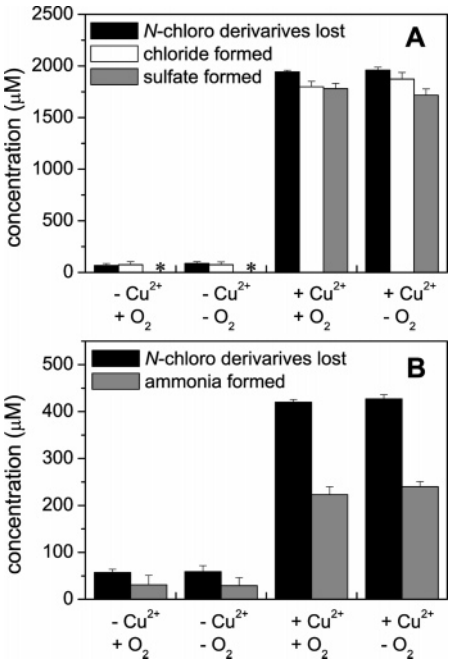

Figure 5. Formation of Cl^-, SO_4^{2-}, and NH_4^+ on decomposition of polymer *N*-chloro derivatives. Samples were analyzed by anion-exchange chromatography (SO_4^{2-} and Cl^-) or cation-exchange chromatography (NH_4^+) with conductivity detection. *N*-Chloro derivatives were determined by assay with TNB. (A) b-HP NCl (1.95 mM) incubated with or without Cu^{2+}(10 μM) under aerobic ($+O_2$) and anoxic ($-O_2$) conditions at 37 °C for 24 h. (B) Same as for (A) except with dnsp-HP chloramines (420 μM). Data are means ± SD of three or more determinations.

close structural analogue of the polymer-derived amidyl radicals.[15]

1,2-Hydrogen shifts of polymer-derived sulfonamidyl radicals would yield $GlcNSO_3$-derived C-2 carbon-centered radicals (Scheme 3). Formation of $SO_3^{\bullet-}$ is attributed to β-scission in these C-2 species (Scheme 3; cf. formation of the $SO_3^{\bullet-}$ from the $GlcNSO_3$ *N*-chlorosulfonamide). 1,5-Hydrogen shifts of the polymer-derived sulfonamidyl radicals and amidyl radicals would yield carbon-centered radicals at the C-4 position of adjacent uronic acid (IdoA and/or GlcA) residues (Scheme 3); the detection of $CO_2^{\bullet-}$ is attributed to β-scission of these C-4 species.

Formation of Sulfate. It has been shown that $SO_3^{\bullet-}$ is generated from the *N*-chlorosulfonamides (see above), and SO_4^{2-} is a known decomposition product of this radical.[23] Formation of this product, and Cl^- ions, from the *N*-chlorosulfonamides was investigated by anion-exchange chromatography with conductivity detection. Decomposition of b-HP NCl (99% *N*-chlorosulfonamides) by Cu^{2+} at 37 °C gave rise to SO_4^{2-} (and Cl^- from one-electron reduction of the *N*-chloro derivatives; Scheme 1) in near quantitative yield with respect to loss of *N*-chloro derivatives (Figure 5A); similar data were obtained with p-HP NCl (95% *N*-chlorosulfonamides). Exclusion of oxygen did not affect the yields of SO_4^{2-}. Only low concentrations of SO_4^{2-} were detected in the absence of added Cu^{2+}, which is consistent with the low extent of *N*-chloro derivative decomposition under these conditions. Decomposition of p-HP NCl by Cu^+ at 22 °C under anoxic conditions also resulted in the formation of SO_4^{2-} in high yield (ca. 60% with respect to loss of *N*-chloro derivatives; data not shown). SO_4^{2-} was not formed in significant concentration upon reaction of the parent polymers with Cu^{2+} or Cu^+ under the above conditions.

Formation of SO_4^{2-} upon decomposition of the polymer *N*-chlorosulfonamides is attributed to oxidation of $SO_3^{\bullet-}$. This may occur via direct metal-ion-mediated one-electron oxidation or, under aerobic conditions, via reaction with O_2 and the formation of $SO_5^{\bullet-}$.[23]

Addition of O_2 to the $GlcNSO_3$-derived C-2 carbon-centered radicals that yield $SO_3^{\bullet-}$ might be expected to compete with the reactions that generate SO_4^{2-}. The lack of an effect of O_2 suggests that release of $SO_3^{\bullet-}$ from the C-2 species is very rapid and competes effectively with peroxyl radical formation; the trapping of $SO_3^{\bullet-}$ by MNP in similar yield (as judged by EPR signal intensities) under aerobic and anoxic conditions supports this proposal. The high yield of SO_4^{2-} indicates that rearrangement of the initial sulfonamidyl radicals via 1,2-shifts and β-scission of the resulting $GlcNSO_3$-derived C-2 carbon-centered radicals (Scheme 3) is the major reaction pathway in this system. The fragments generated via this pathway would have lower charge density than oligosaccharides generated via enzymatic cleavage and might therefore be expected to have lower electrophoretic mobility on polyacrylamide gels; this would result in an underestimation of the yield of strand breaks (see Formation of Strand Breaks section).

Formation of Ammonia. Evidence has been obtained for the formation of C-2 imines in high yield from the polymer-derived *N*-chlorosulfonamides (see above). Structurally identical C-2 imines may be generated from the polymer-derived chloramines via one-electron oxidation of intermediate $GlcNH_2$-derived C-2 carbon-centered radicals by transition-metal ions or by O_2 (i.e., $C^{\bullet}-NH_2 + M^{n+} \rightarrow C{=}NH + M^{(n-1)+} + H^+$ or $C^{\bullet}-NH_2 + O_2 \rightarrow C(OO^{\bullet})-NH_2 \rightarrow C{=}NH + O_2^{\bullet-} + H^+$). As these C-2 imines formed from the polymer-derived *N*-chlorosulfonamides and chloramines might be expected to hydrolyze to the corresponding C-2 ketones and ammonia (NH_4^+), the formation of the latter was investigated by cation-exchange chromatography with conductivity detection.

A. *N*-Chlorosulfonamides. Decomposition of p-HP NCl (95% *N*-chlorosulfonamides) by Cu^{2+} (10 μM) at 37 °C (cf. Figure 1B and Figure 2B) did not result in the detection of NH_4^+ (data not shown). These data suggest that the polymer C-2 imines do not hydrolyze to the corresponding C-2 ketones and that alternative reactions of these species must lead to the fragmentation detected with the polymer-derived *N*-chlorosulfonamides.

B. Chloramines. NH_4^+ was detected in ca. 50% yield with respect to loss of *N*-chloro derivatives upon decomposition of dnsp-HP chloramines by Cu^{2+} (10 μM) at 37 °C (Figure 5). In the absence of added Cu^{2+}, much lower concentrations were detected, consistent with the low extent of chloramine decomposition under these conditions. As the data obtained with the polymer-derived *N*-chlorosulfonamides demonstrate that C-2 imines do not yield NH_4^+, formation of this product from the polymer-derived chloramines is unlikely to occur via oxidation of intermediate $GlcNH_2$-derived C-2 carbon-centered radicals to C-2 imines. These C-2 radicals may undergo alternative acid-/base-catalyzed rearrangement that results in loss of the C-1 glycosidic substituent (i.e., $C(OR)H-C^{\bullet}-NH_2 \rightarrow C^{\bullet}H-C{=}NH_2 + HOR$) (cf. related reactions in refs 24 and 25). The uronic-acid-derived C-4 carbon-centered radicals generated from the

(23) Neta, P.; Huie, R. E. *Environ. Health Perspect.* **1985**, *64*, 209−217.

chloramines have been shown to yield $CO_2^{\bullet-}$ via β-scission (Scheme 3), and they may also undergo other rearrangements that involve cleavage of the glycosidic bond (e.g., β-scission, C−O−C$^{\bullet}$ → C$^{\bullet}$ + O═C; cf. evidence for fragmentation of hyaluronan and chondroitin sulfate via β-scission of uronic-acid-derived C-4 carbon-centered radicals[15]). Modifications arising from one or more of the abovementioned rearrangements are believed to ultimately yield NH_4^+ and would also account for the occurrence of polymer fragmentation.

C. Dichloramines. Incubation of dnsp-HP dichloramines (2.56 mM) at 37 °C for 24 h in the absence of added metal ions resulted in the formation of NH_4^+ in ca. 5% yield with respect to loss of *N*-chloro derivatives (ca. 9% yield with respect to dichloramine functions); addition of Cu^{2+} (10 μM), which did not affect the rate or extent of decomposition, did not affect the yield of NH_4^+.

Formation of Chromophoric Products. To further characterize the polymer modifications that are consequent upon decomposition of the *N*-chloro derivatives, reaction mixtures were analyzed by UV−vis spectroscopy.

A. *N*-Chlorosulfonamides. Decomposition of the polymer-derived *N*-chlorosulfonamides (p-HP NCl and b-HP NCl) by Cu^{2+} at 37 °C resulted in the generation of optical absorbances over a wide range of wavelengths (Figure 6B, Supporting Information); comparable data were obtained from aerobic and anoxic incubations. The most intense absorbance had a peak with λ_{max} = ca. 270 nm. The rate of formation of this peak correlated closely with the rate of decomposition of the *N*-chloro derivatives (cf. Figure 1B) and the rate of polymer fragmentation (cf. Figure 2B). After decomposition of the *N*-chloro derivatives was complete, a loss of a shoulder of absorbance at ca. 295 nm and an accumulation of absorbance at longer wavelengths were observed. No absorbance changes were detected upon incubation of the polymer *N*-chloro derivatives alone or from the parent polymers in the presence or absence of Cu^{2+}.

The C-2 imines formed upon decomposition of the *N*-chloro sulfonamides (Scheme 3) are believed to be the source of the species which gives rise to the absorbance peak at λ_{max} = ca. 270 nm. Evidence has been obtained that these imines do not hydrolyze to the corresponding ketones (see above). A likely alternative reaction of these species, which can account for the observed chromophores and polymer fragmentation, is tautomerization to an enamine(ol) and subsequent elimination of the C-1 glycosidic substituent via reverse Michael addition (Scheme 4). Fragmentation in this fashion, via an enamine(ol) intermediate, has been observed previously with a 3-oxo-2-amino glycoside.[26] The α,β-unsaturated derivatives formed via these rearrangements are believed to be responsible for the absorbance peak with λ_{max} = ca. 270 nm. Alternate reaction pathways are likely to underlie the formation of the species that give rise to the shoulder of absorbance at ca. 295 nm as the formation and subsequent loss of this species appear to be independent of the formation of the absorbance peak with λ_{max} = ca. 270 nm.

B. Chloramines. Decomposition of the polymer-derived chloramines (dnsp-HP chloramines and p-HS NCl chloramine) by Cu^{2+} under aerobic and anoxic conditions gave rise to absorbances over a wide range of wavelengths (Figure 6A, Supporting Information); very similar data were obtained from aerobic and anoxic incubations. In contrast to the *N*-chlorosulfonamides, selective formation of an absorbance peak with λ_{max} = ca. 270 nm was not observed. The rate of chromophore formation correlated closely with the rate of chloramine decomposition (cf. Figure 1A) and the rate of polymer fragmentation (cf. Figure 2A). No absorbance changes were detected upon incubation of the polymer-derived chloramines alone or from the parent polymers in the presence or absence of Cu^{2+}.

Scheme 4. Proposed Mechanism for the Formation of Strand Breaks from Polymer-Derived C-2 Imines

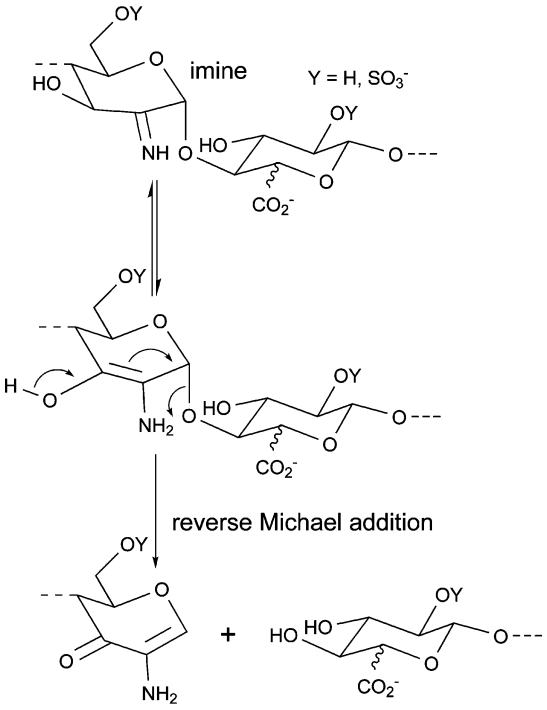

As previously discussed, decomposition of the polymer-derived chloramines could yield C-2 imines; however, this should give rise to an absorbance peak with λ_{max} = 270 nm (cf. data obtained with the *N*-chlorosulfonamides) and this was not observed. Thus, it is believed that the observed chromophores are generated via reactions of $GlcNH_2$-derived C-2 carbon-centered radicals that do not yield C-2 imines or via reactions of uronic-acid-derived C-4 carbon-centered radicals (possibly via the reaction mechanisms discussed in the previous section).

C. Dichloramines. Decomposition of the polymer-derived dichloramines in the absence of added agents results in rapid, complex absorbance changes and, ultimately, in the formation of a chromophore with λ_{max} = 331 nm.[14] As a result of this "background" chromophore formation, a contribution from metal-ion-mediated pathways could not be determined.

Conclusions

It has been shown here that polymer-bound *N*-chloro derivatives formed on heparan sulfate, via reaction with HOCl, are readily decomposed by both transition-metal ions (Cu^+, Cu^{2+}, and Fe^{2+}) and superoxide radicals ($O_2^{\bullet-}$). These reactions result in polymer fragmentation via the initial formation of nitrogen-

(24) Davies, M. J.; Gilbert, B. C. In *Advances in Detailed Reaction Mechanisms*; JAI Press: 1991; Vol. 1, pp 35−81.
(25) Beckwith, A. L. J.; Crich, D.; Duggan, P. J.; Yao, Q. *Chem. Rev.* **1997**, *97*, 3273−3312.
(26) Liu, H. M.; Xu, W.; Liu, Z. Z. *Carbohydr. Res.* **2001**, *331*, 229−232.

centered radicals generated by reductive homolysis of the N−Cl bonds (Scheme 1).

Cu^{+} and Fe^{2+} promoted rapid decomposition of the polymer-derived chloramines (R−NCl−H), dichloramines ($R-NCl_2$), and *N*-chlorosulfonamides ($R-NCl-SO_3^-$). Cu^{2+} catalyzed slow decomposition of polymer-derived chloramines and *N*-chlorosulfonamides. With Cu^{2+}, decomposition may occur via direct reaction with Cu^{2+} or via the formation of Cu^{+}. $O_2^{\bullet-}$, generated by SOTS-1, also promoted decomposition of polymer-derived *N*-chlorosulfonamides and chloramines, though decomposition of the latter species was relatively inefficient. Metal ion chelators strongly inhibited these $O_2^{\bullet-}$-mediated decomposition reactions, suggesting that they are catalyzed by (trace) redox-active metal ions (Scheme 1).

Radicals generated upon one-electron reduction of the polymer *N*-chloro derivatives and the corresponding monosaccharide *N*-chloro derivatives have been detected and characterized by EPR spin trapping using DMPO and MNP. The spin adducts detected have been attributed to the trapping (i) of the initial nitrogen-centered radicals, (ii) of carbon-centered radicals generated via hydrogen atom abstraction reactions of these species, and (iii) of species generated via rearrangement of the carbon-centered radicals, i.e., $CO_2^{\bullet-}$ and $SO_3^{\bullet-}$.

The EPR signals detected on decomposition of the $GlcNH_2$ chloramine and the $GlcNSO_3$ *N*-chlorosulfonamide have been assigned to adducts of C-2 carbon-centered radicals. The formation of these radicals has been ascribed to the occurrence of 1,2-hydrogen atom shifts to initial (undetected) aminyl radicals (R−N•−H) and sulfonamidyl radicals ($R-N^{\bullet}-SO_3^-$) (Scheme 2). Although aminyl 1,2-hydrogen atom shifts are known,[27] sulfonamidyl 1,2-hydrogen shifts have not previously been reported. As with the closely related alkoxyl 1,2-hydrogen shift,[28] both of these rearrangements are likely to be assisted by water molecules. The formation of $SO_3^{\bullet-}$ on decomposition of $GlcNSO_3$ NCl is attributed to β-scission of the $GlcNSO_3$ C-2 carbon-centered radical (Scheme 2). β-Scission reactions of carbon-centered radicals to give heteroatom-centered radicals are well-known (e.g., ref 29), although the authors are unaware of any previous examples that yield $SO_3^{\bullet-}$. With the $GlcNH_2$ dichloramine, the initially formed *N*-chloroaminyl radical (R−N•−Cl) was the only species detected.

The high-molecular mass species detected upon decomposition of the polymer-derived chloramines, *N*-chlorosulfonamides, and chloramides in the presence of MNP and DMPO have been assigned to adducts of polymer-derived carbon-centered radicals. These species are believed to be glycosamine-derived C-2 carbon-centered radicals and/or uronic-acid-derived C-4 carbon-centered radicals formed via 1,2- and 1,5-hydrogen shifts to the initially formed polymer-derived nitrogen-centered radicals (Scheme 3).

Indirect evidence for the formation of glycosamine-derived C-2 carbon-centered radicals and uronic-acid-derived C-4 carbon-centered radicals arises from the detection of $SO_3^{\bullet-}$ and $CO_2^{\bullet-}$ upon decomposition of polymer *N*-chloro derivatives. $SO_3^{\bullet-}$ was detected upon decomposition of polymer-derived *N*-chlorosulfonamides; generation of this radical is attributed to β-scission of $GlcNSO_3$-derived C-2 carbon-centered radicals that are formed via 1,2-hydrogen shifts to initial $GlcNSO_3$-derived sulfonamidyl radicals (Scheme 3). $CO_2^{\bullet-}$ was detected upon decomposition of polymer-derived chloramines, *N*-chlorosulfonamides, and chloramides; generation of this radical is attributed to β-scission reactions of uronic-acid-derived C-4 carbon-centered radicals that are formed via 1,5-hydrogen shifts to initial aminyl, sulfonamidyl, and amidyl radicals (Scheme 3). Evidence has previously been obtained that $CO_2^{\bullet-}$ is generated via analogous reactions initiated by amidyl radicals formed on hyaluronan and chondroitin sulfate.[15]

Decomposition of polymer-derived *N*-chlorosulfonamides resulted in the formation of SO_4^{2-} in near quantitative yield and the formation of UV−vis chromophores. Formation of SO_4^{2-} is attributed to further reactions of $SO_3^{\bullet-}$. As formation of $SO_3^{\bullet-}$ involves formation of polymer-derived C-2 imines (Scheme 3), it follows that these species are formed in near quantitative yield upon decomposition of polymer-derived *N*-chlorosulfonamides and are key intermediates in the formation of strand breaks and the UV−vis chromophores. It has been shown that the C-2 imines do not hydrolyze to yield NH_4^+ under the conditions employed. Instead, it is proposed that the C-2 imines tautomerize and eliminate the C-1 glycosidic substituent via reverse Michael addition (Scheme 4). This process can account for the occurrence of polymer fragmentation and the formation of the UV−vis chromophores. The intermediacy of the C-2 imines in the mechanism of polymer fragmentation is noteworthy: in the generally accepted mechanisms of radical-mediated polysaccharide fragmentation, strand scission has been proposed to occur via direct rearrangement of radicals formed on the polymer backbone rather than heterolytic transformations of nonradical lesions.[30] Pathways of the latter type may have more general significance than is currently appreciated: ketones generated upon one-electron oxidation of α-hydroxyalkyl radicals should also be susceptible to tautomerization/elimination reactions that result in glycosidic bond cleavage.

Decomposition of polymer-derived chloramines resulted in the formation of NH_4^+ and the formation of UV−vis chromophores, which were different from those detected with the *N*-chlorosulfonamides. Although evidence has been obtained that the polymer-derived aminyl radicals undergo 1,5-shifts and may undergo 1,2-shifts, the relative importance of these rearrangements is uncertain. It is proposed that one or both of these processes, which generate $GlcNH_2$-derived C-2 carbon-centered radicals and uronic-acid-derived C-4 carbon-centered radicals, ultimately yield strand breaks, NH_4^+, and the observed chromophores. The $GlcNH_2$-derived C-2 carbon-centered radicals could give rise to strand scission via acid-/base-catalyzed radical rearrangement that results in elimination of the C-1 glycosidic substituent.[24,25] As the chloramine-derived chromophores are different from those formed from the *N*-chlorosulfonamides, it appears that C-2 imines (which could be formed via oxidation of $GlcNH_2$-derived C-2 carbon-centered radicals) are not important intermediates in product formation from the chloramines. The uronic-acid-derived C-4 carbon-centered radicals could give rise to cleavage of the adjacent glycosidic bonds via direct rearrangement or via reaction with O_2 and reactions initiated by the resultant peroxyl radicals. Evidence has previously been obtained that uronic-acid-derived C-4 carbon-centered radicals formed on hyaluronan and chondroitin sulfate give rise to

(27) Anderson, N. H.; Norman, R. O. C. *J. Chem. Soc. B* **1971**, 993−1003.
(28) Konya, K. G.; Paul, T.; Lin, S.; Janusz, L.; Ingold, K. U. *J. Am. Chem. Soc.* **2000**, *122*, 7518−7527.
(29) Kim, S.; Cheong, J. H. *Chem. Commun.* **1998**, *10*, 1143−1144.
(30) von Sonntag, C. *Adv. Carbohydr. Chem. Biochem.* **1980**, *37*, 7−77.

polymer fragmentation via β-scission and competing O_2-dependent processes.[15]

The *N*-chloroaminyl radicals generated via one-electron reduction of the polymer-derived dichloramines are also likely to initiate polymer fragmentation via hydrogen atom abstraction, though the carbon-centered radicals generated via such reactions were not observed. Rearrangement of the *N*-chloroaminyl radicals via 1,5-hydrogen shifts would yield uronic-acid-derived C-4 carbon-centered radicals and, upon β-scission of these species, $CO_2^{\bullet-}$. As $CO_2^{\bullet-}$ was not observed, this suggests that the 1,5-shift rearrangement does not compete efficiently with other reactions of the parent radical. Dichloramine decomposition in the absence of added agents, which is the subject of ongoing studies, is believed to occur via a nonradical process.

The production of HOCl in vivo by MPO is likely to be localized to the negatively charged glycosaminoglycans of the extracellular matrix and cell surfaces because of their association with the highly positively charged MPO protein.[13] Heparan sulfate proteoglycans are key components of vascular basement membranes and cell surfaces and are likely to be targets for oxidation by MPO-derived HOCl in a variety of inflammatory milieu. The degradation of heparan sulfate by HOCl, which involves the initial generation of *N*-chloro derivatives, may contribute to pathology in a number of inflammatory diseases in which a role for MPO-mediated tissue damage has been implicated, such as heart disease[31] and kidney disease.[32] Transition-metal ions and $O_2^{\bullet-}$ may play an important role in inflammation-induced tissue injury by promoting decomposition of the *N*-chloro derivatives of heparan sulfate to nitrogen-centered radicals and initiating polymer modification and fragmentation. Similar degradation processes involving other biological macromolecules that yield *N*-chloro derivatives upon reaction with HOCl may also be important, with evidence having been presented for reaction of transition-metal ions and $O_2^{\bullet-}$ with *N*-chloro derivatives formed on proteins and the *N*-acetylated glycosaminoglycans hyaluronan and chondroitin sulfate giving rise to fragmentation of their polymer backbones.[15,18,33,34]

Acknowledgment. We thank the Australian Research Council for support under the ARC Centres of Excellence Program and the National Health and Medical Research Council for financial support. The authors also gratefully acknowledge the provision of SOTS-1 by Prof. Chris Easton (Research School of Chemistry, Australian National University, Canberra).

Supporting Information Available: Two tables containing hyperfine coupling constants of spin adduct data obtained using DMPO (Table 1) and MNP (Table 2) as spin traps and UV−vis absorbance spectra of chromophores generated during decomposition of polymer-derived *N*-chloro derivatives (pdf files). This material is available free of charge via the Internet at http://pubs.acs.org.

JA0577239

(31) Nicholls, S. J.; Hazen, S. L. *Arterioscler. Thromb. Vasc. Biol.* **2005**, *25*, 1102−1111.
(32) Malle, E.; Buch, T.; Grone, H. J. *Kidney Int.* **2003**, *64*, 1956−1967.
(33) Hawkins, C. L.; Davies, M. J. *Biochem. J.* **1998**, *332*, 617−625.
(34) Hawkins, C. L.; Rees, M. D.; Davies, M. J. *FEBS Lett.* **2002**, *510*, 41−44.